



Wireless Attacks on Aircraft Instrument Landing Systems

Harshad Sathaye, Domien Schepers, Aanjhan Ranganathan, and
Guevara Noubir, *Northeastern University*

<https://www.usenix.org/conference/usenixsecurity19/presentation/sathaye>

**This paper is included in the Proceedings of the
28th USENIX Security Symposium.**

August 14–16, 2019 • Santa Clara, CA, USA

978-1-939133-06-9

**Open access to the Proceedings of the
28th USENIX Security Symposium
is sponsored by USENIX.**

Wireless Attacks on Aircraft Instrument Landing Systems

Harshad Sathaye, Domien Schepers, Aanjhan Ranganathan, and Guevara Noubir
Khoury College of Computer Sciences
Northeastern University, Boston, MA, USA

Abstract

Modern aircraft heavily rely on several wireless technologies for communications, control, and navigation. Researchers demonstrated vulnerabilities in many aviation systems. However, the resilience of the aircraft landing systems to adversarial wireless attacks have not yet been studied in the open literature, despite their criticality and the increasing availability of low-cost software-defined radio (SDR) platforms. In this paper, we investigate the vulnerability of aircraft instrument landing systems (ILS) to wireless attacks. We show the feasibility of spoofing ILS radio signals using commercially-available SDR, causing last-minute *go around* decisions, and even missing the landing zone in low-visibility scenarios. We demonstrate on aviation-grade ILS receivers that it is possible to fully and in fine-grain control the course deviation indicator as displayed by the ILS receiver, in *real-time*. We analyze the potential of both an overshadowing attack and a lower-power single-tone attack. In order to evaluate the complete attack, we develop a tightly-controlled closed-loop ILS spoofer that adjusts the adversary's transmitted signals as a function of the aircraft GPS location, maintaining power and deviation consistent with the adversary's target position, causing an undetected off-runway landing. We systematically evaluate the performance of the attack against an FAA certified flight-simulator (X-Plane)'s AI-based autoland feature and demonstrate systematic success rate with offset touch-downs of 18 meters to over 50 meters.

1 Introduction

Today, the aviation industry is experiencing significant growth in air traffic with more than 5000 flights [14] in the sky at any given time. It has become typical for air traffic control towers to handle more than a thousand takeoffs and landings every day. For example, Atlanta's Hartsfield-Jackson International airport handles around 2500 takeoffs and landings every day. Boston's Logan airport which is not one of the busiest airports in the world managed an average of 1100 flights every day in August 2018. The modern aviation ecosystem heavily relies on a plethora of wireless technologies for their safe

and efficient operation. For instance, air traffic controllers verbally communicate with the pilots over the VHF (30 to 300 MHz) radio frequency channels. The airplanes continuously broadcast their position, velocity, callsigns, altitude, etc. using the automatic dependent surveillance-broadcast (ADS-B) wireless communication protocol. Primary and secondary surveillance radars enable aircraft localization and provide relevant target information to the air traffic controllers. Traffic Alert and Collision Avoidance System (TCAS), an airborne wireless system independent of the air traffic controller enables the aircraft to detect potential collisions and alert the pilots. Air traffic information, flight information and other operational control messages between the aircraft and ground stations are transferred using the Aircraft Communications Addressing and Reporting System (ACARS) which uses the VHF and HF radio frequency channels for communication. Similarly, many radio navigation aids such as GPS, VHF Omnidirectional Radio Range (VOR), Non-directional radio beacons (NDB), Distance Measuring Equipment (DME), and Instrument Landing System (ILS) play crucial roles during different phases of an airplane's flight.

Many studies have already demonstrated that a number of the above-mentioned aviation systems are vulnerable to attacks. For example, researchers [22] injected non-existing aircraft in the sky by merely spoofing ADS-B messages. Some other attacks [37] modified the route of an airplane by jamming and replacing the ADS-B signals of specific victim aircraft. ACARS, the data link communications system between aircraft and ground stations was found to leak a significant amount of private data [50], e.g., passenger information, medical data and sometimes even credit card details were transferred. GPS, one of the essential navigation aids is also vulnerable to signal spoofing attacks [32]. Furthermore, an attacker can spoof TCAS messages [42] creating false resolution advisories and forcing the pilot to initiate avoidance maneuvers. Given the dependence on wireless technologies, the threats described above are real and shows the importance of building secure aviation control, communication and navigation systems.

One of the most critical phases of an airplane’s flight plan is the final approach or landing phase as the plane descends towards the ground actively maneuvered by the pilot. For example, 59% of the fatal accidents documented by Boeing [16] occurred during descent, approach and landing. Several technologies and systems such as GPS, VOR, DME assist the pilot in landing the aircraft safely. The Instrument Landing System (ILS) [17] is today the de-facto approach system used by planes at a majority of the airports as it is the most precise system capable of providing accurate horizontal and vertical guidance. At Boston’s Logan International Airport, 405,822 [1] flight plans were filed in 2017. Out of these 405,822 flight plans, 95% were instrument flight rule (IFR) plans. Instrument flight rules are a set of instructions established by the FAA to govern flight under conditions in which flying by visual reference is either unsafe or just not allowed. Also, several European airports [9] prohibit aircraft from landing using visual flight rules during the night. ILS incorporates radio technology to provide all-weather guidance to pilots which ensures safe travel and any interference can be catastrophic.

As recently as September 2018, the pilots of Air India flight AI-101 reported an instrument landing system (ILS) malfunction and were forced to do an emergency landing. Even worse, TCAS, ACARS, and a majority of other systems that aid a smooth landing were unusable. Furthermore, NASA’s Aviation Safety Reporting System [25] indicate over 300 ILS related incidents where pilots reported the erratic behavior of the localizer and glideslope—two critical components of ILS. ILS also plays a significant role in autoland systems that are capable of landing aircraft even in the most adverse conditions without manual interference. Autoland systems have significantly advanced over the years since its first deployment in De Havilland’s DH121 Trident, the first airliner to be fitted with an autoland system [15]. However, several near-catastrophic events [4, 8, 12] have been reported due to the failure or erratic behavior of these autoland systems with ILS interference as one of the principal causes. With increasing reliance on auto-pilot systems and widespread availability of low-cost software-defined radio hardware platforms, adversarial wireless interference to critical infrastructure systems such as the ILS cannot be ruled out.

In this work, we investigate the security of aircraft instrument landing system against wireless attacks. To the best of our knowledge, there has been no prior study on the security guarantees of the instrument landing system. Specifically, our contributions are as follows.

- We analyze the ILS localizer and glideslope waveforms, the transmitters and receivers, and show that ILS is vulnerable to signal spoofing attacks. We devise two types of wireless attacks i) overshadow, and ii) single-tone attacks.
- For both the attacks, we generate specially crafted radio signals similar to the legitimate ILS signals using

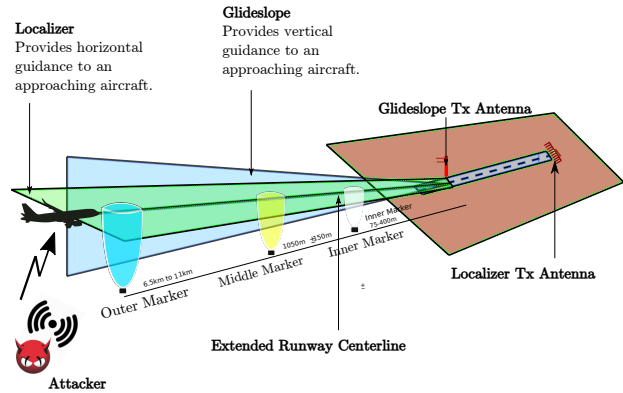


Figure 1: Overview of ILS sub-systems. The ILS consists of three subsystems: i) Localizer, ii) glideslope, and (iii) marker beacons.

low-cost software-defined radio hardware platform and successfully induce aviation-grade ILS receivers, in *real-time*, to lock and display arbitrary alignment to both horizontal and vertical approach path. This demonstrates the potential for an adversary to the least be able to trigger multiple aborted landings causing air traffic disruption, and in the worst case, cause the aircraft to overshoot the landing zone or miss the runway entirely.

- In order to evaluate the complete attack, we develop a tightly-controlled closed-loop ILS spoofer. It adjusts the the adversary’s transmitted signals as a function of the aircraft GPS location, maintaining power and deviation consistent with the adversary’s target position, causing an undetected off-runway landing. We demonstrate the integrated attack on an FAA certified flight-simulator (X-Plane), incorporating a spoofing region detection mechanism, that triggers the controlled spoofing on entering the landing zone to reduce detectability.
- We systematically evaluate the performance of the attack against X-Plane’s AI-based autoland feature, and demonstrate the systematic success rate with offset touchdowns of 18 meters to over 50 meters.
- We discuss potential countermeasures including failsafe systems such as GPS and show that these systems also do not provide sufficient security guarantees. We highlight that implementing cryptographic authentication on ILS signals is not enough as the the system would still be vulnerable to record and replay attacks. Therefore, through this research, we highlight an open research challenge of building secure, scalable and efficient aircraft landing systems.

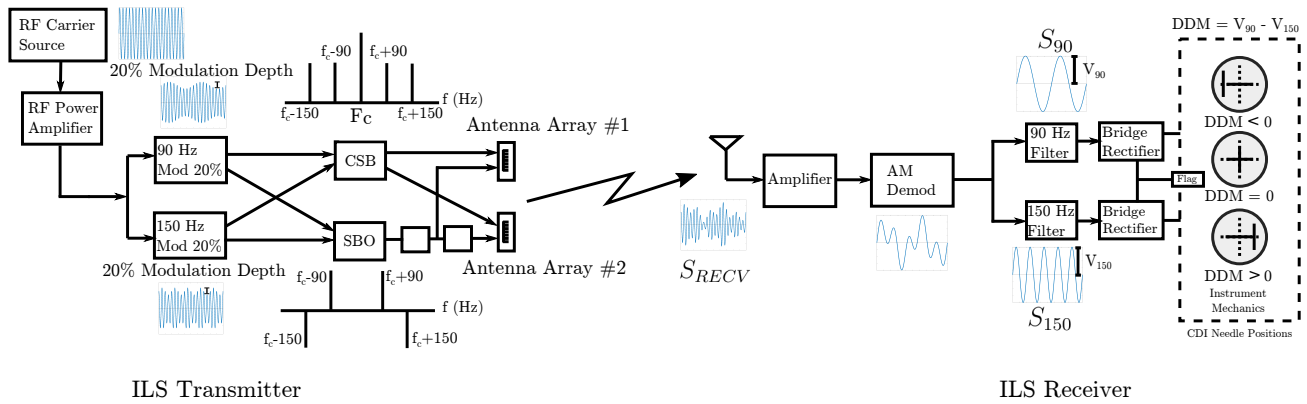


Figure 2: Block diagram of ILS transmitter and receiver describing the process of generation and reception of ILS signal along with waveforms at each stage.

2 Background

Approach systems enable pilots to land airplanes even in extreme weather conditions and are classified into non-precision and precision approach systems based on the accuracy and type of approach guidance provided to an aircraft. Non-precision approach systems provide only horizontal or lateral guidance (heading/bearing). Examples of non-precision approach systems are VHF Omnidirectional Range (VOR) [58], Non-Directional Beacon (NDB) [57], and satellite systems such as GPS. With the development of precision approach systems, the use of non-precision approach systems such as VOR and NDB has significantly decreased today. Precision approach systems provide both horizontal (heading/bearing) as well as vertical (glide path) guidance to an approaching aircraft. The Instrument Landing System (ILS) is the most commonly deployed precision approach system in use today. Other examples of precision approach systems include Microwave Landing System (MLS), Transponder Landing System (TLS), Ground Based Augmentation Landing System (GLS), and Joint Precision Approach and Landing System (JPALS). It is important to note that these alternate landing systems fundamentally still use existing ILS concepts and equipment mostly in scenarios where ILS is unavailable. For example, TLS enables precision landing guidance in places where the terrain is uneven, and the ILS signal reflections off the ground cause undesirable needle deflections by *emulating* the ILS signals using only one base tower (in contrast to two for ILS) whose placement allows more flexibility. However, TLS still leverages the same fundamental concepts of ILS. In short, ILS plays a key, de-facto role in providing precision landing guidance at the majority of airports today and it is, therefore, essential to evaluate its resilience to modern-day cyber-physical attacks.

2.1 Instrument Landing System (ILS)

The first fully operational ILS was deployed in 1932 at the Berlin Tempelhof Central Airport, Germany. ILS enables the pilot to align the aircraft with the centerline of the runway and maintain a safe descent rate. ITU defines ILS [28] as “a radio navigation system which provides aircraft with horizontal and vertical guidance just before and during landing and at certain fixed points, indicates the distance to the reference point of landing”. Autopilot systems on some modern aircraft [49] use ILS signals to execute a fully autonomous approach and landing, especially in low visibility settings. ILS (Figure 1) comprises of three independent subsystems: i) localizer, ii) glideslope and iii) marker beacons. The localizer and the glideslope guide the aircraft in the horizontal and vertical plane respectively. The marker beacons act as checkpoints that enable the pilot to determine the aircraft’s distance to the runway. ILS has three operational categories: i) CAT I, ii) CAT II and, iii) CAT III. CAT III further has three sub-standards IIIa, IIIb and, IIIc. These operational categories are decided based on ILS installations at the airport ¹ and is independent of the receiver on the aircraft. With the advent of GPS and other localization technologies, the marker beacons are less important today and increasingly obsolete. However, the localizer and the glideslope play a major role in an aircraft’s safe landing today and is expected to remain so for many years.

2.1.1 ILS Signal Generation

ILS signals are generated and transmitted such that the waves form a specific radio frequency signal pattern in space to create guidance information related to the horizontal and vertical

¹Procedures for the Evaluation and Approval of Facilities for Special Authorization Category I Operations and All Category II and III Operations http://fsims.faa.gov/wdocs/Orders/8400_13.htm

positioning. ILS signal generators leverage *space modulation* i.e., use multiple antennas to transmit an amplitude modulated radio frequency signals with various powers and phases. The transmitted signals combine in the airspace to form signals with different depths of modulation (DDM) at various points within the 3D airspace. Each DDM value directly indicates a specific deviation of the aircraft from the correct touchdown position. For example, the signals combine in space to produce a signal with zero difference in the depth of modulation (DDM) along the center-line of the runway. It is important to note that unlike traditional modulation techniques where the modulation occurs within the modulating hardware, in space modulation, the signals mix within the airspace.

The process of generating the localizer and glideslope signals (Figure 2) are similar with differences mainly in the carrier frequency used and how they are combined in space to provide the relevant guidance information. The carrier signal is amplitude modulated with 90 Hz and 150 Hz tones to a certain depth of modulation. The depth of modulation or modulation index is the measure of the extent of amplitude variation about an un-modulated carrier. The depth of modulation is set at 20% and 40% respectively for localizer and glideslope signals. The output of both the 90 Hz and 150 Hz modulator is then combined to yield two radio frequency signals: a carrier-plus-sidebands (CSB) and a sidebands-only (SBO) signal. The names of the signal directly reflect their spectral energy configuration with the CSB containing both the sideband energy and the assigned carrier frequency while in the SBO signal the carrier frequency component is suppressed. The CSB and SBO signals are subjected to specific phase shifts before being transmitted. The phase shifts are carefully chosen such that when the CSB and SBO signals combine in space, the resulting signal enables the aircraft to determine its horizontal and vertical alignment with the approach path.

Localizer. The localizer subsystem consists of an array of multiple antennas that emit the CSB and SBO signals such that the 150 Hz modulation predominates to the right of the runway centerline and the 90 Hz signal prevails to the left. In other words, if the flight is aligned to the right of the runway during the approach, the 150 Hz dominant signal will indicate the pilot to steer left and vice versa. The antenna array of the localizer is located at the opposite end (from the approach side) of the runway. Each runway operates its localizer at a specific carrier frequency (between 108.1 MHz to 111.95 MHz) and the ILS receiver automatically tunes to this frequency as soon as pilot inputs the runway identifier in the cockpit receiver module. Additionally, the runway identifier is transmitted using a 1020 Hz morse code signal over the localizer's carrier frequency.

Glideslope. The glideslope subsystem uses two antennas to create a signal pattern similar to that of the localizer except on a vertical plane. The two antennas are mounted on a tower

at specific heights defined by the glide-path angle suitable for that particular airport's runway. In contrast to the localizer, the glideslope produces the signal pattern in the airspace based on the sum of the signals received from each antenna via the direct line-of-sight path and the reflected path. The mixing of the CSB and SBO signals results in a pattern in which the 90 Hz component of the signal predominates in the region above the glide-path while the 150 Hz prevails below the glide-path. The glideslope uses carrier frequencies between 329.15 MHz and 335.0 MHz, and the antenna tower is located near the touchdown zone of the runway. Typically, the center of the glide-slope defines a glide path angle of approximately 3°. For every localizer frequency, the corresponding glideslope frequency is hardcoded i.e., the localizer-glideslope frequencies occur in pairs and the instrument automatically tunes to the right glideslope frequency when the pilot tunes to a specific runway's localizer frequency.

2.1.2 ILS Receiver

The combined signals received at the aircraft are amplified, demodulated, and filtered to recover the 90 Hz and 150 Hz components. A bridge rectifier is used to convert the amplitude of the recovered tones to DC voltage levels. The DC voltage output is directly proportional to the depth of the modulation of the 90 Hz and 150 Hz tones—a direct measure of the dominating frequency signal. The DC voltage causes the course deviation indicator needle to deflect based on the difference in the depth of the modulation of the two tones thereby precisely indicating the aircraft's lateral and vertical deviation from approach path.

For example, an aircraft that is on-course will receive both 90 and 150 Hz signals with the same amplitude, i.e., equal depth of modulation and will result in zero *difference in the depth of modulation* and therefore cause no needle deflections. However, an aircraft that is off-course and not aligned with the approach path will receive signals with a non-zero difference in the depth of modulation resulting in a corresponding deflection of the needle. The instruments are calibrated to show full scale deflection if $DDM > 0.155$ or $DDM < -0.155$ for localizer and if $DDM > 0.175$ or $DDM < -0.175$ for glideslope [20]. These values correspond to 2.5° offset on the left side of the runway, 2.5° offset on the right side of the runway, 0.7° offset above the glide path angle and 0.7° below the glide path angle respectively.

2.2 Typical Approach Sequence

Pilots use aeronautical charts containing vital information about the terrain, available facilities and their usage guidelines throughout a flight. Approach plates are a type of navigation chart used for flying based on instrument readings. Every pilot is required to abide by the routes and rules defined in an approach plate unless ordered otherwise by the air traffic controller. The approach plate contains information like active localizer frequency of the runway, the runway identifier

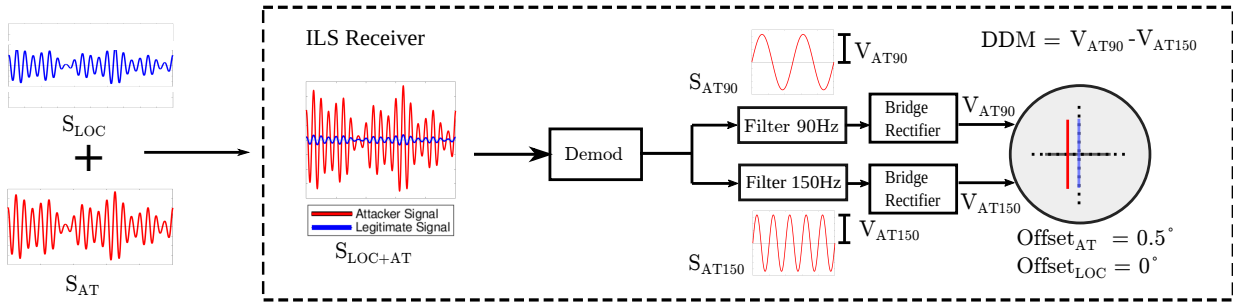


Figure 3: Schematic of the overshadow attack. The attacker’s signal has a preset DDM corresponding to 0.5° to the right of the runway. Attacker’s signal overshadows the legitimate signal. The blue line represents the needle position without attack.

in Morse code, glideslope interception altitude, ATC tower frequencies, and other information crucial for a safe landing.

Once the pilot receives the clearance to land at an assigned runway, the pilot enters the localizer frequency associated with the designated runway and enters the course of the runway into the auto-pilot. Note that the localizer and glideslope frequencies occur in pairs and therefore the pilot does not have to manually enter the corresponding glideslope frequency. When the pilot intercepts the localizer, the course deviation indicator needle is displayed on the cockpit. The pilot then verifies whether the receiver is tuned to the right localizer by confirming the runway identifier which is transmitted as morse code on the localizer frequency. For example, for landing on runway 4R (Runway Ident - IBOS) at Logan International Airport, Boston, the pilot will tune to 110.3 MHz and will verify this by confirming the Morse code: .. / -... / --- / ... Based on the deviation of the aircraft from the runway and the approach angle, the indicator will guide the pilot to appropriately maneuver the aircraft. Modern autopilot systems are capable of receiving inputs from ILS receivers and autonomously land the aircraft without human intervention.

In fact, pilots are trained and instructed to trust the instruments more than their intuition. If the instruments ask them to fly right, the pilots will fly right. This is true specifically when flying in weather conditions that force the pilots to follow the instruments. Detecting and recovering from any instrument failures during crucial landing procedures is one of the toughest challenges in modern aviation. Given the heavy reliance on ILS and instruments in general, malfunctions and adversarial interference can be catastrophic especially in autonomous approaches and flights. In this paper, we demonstrate vulnerabilities of ILS and further raise awareness towards the challenges of building secure aircraft landing systems.

3 Wireless Attacks on ILS

We demonstrate two types of wireless attacks: i) Overshadow attack and ii) Single-tone attack. In the overshadow attack, the attacker transmits pre-crafted ILS signals of higher signal strength; thus overpowering the legitimate ILS signals. The

single-tone attack is a special attack where it is sufficient for the attacker to transmit a single frequency tone signal at a specific signal strength (lower than the legitimate ILS signal strength) to interfere and control the deflections of the course deviation indicator needle.

Attacker model. We make the following assumptions regarding the attacker. Given that the technical details of ILS are in the public domain, we assume that the attacker has complete knowledge of the physical characteristics of ILS signals e.g., frequencies, modulation index etc. We also assume that the attacker is capable of transmitting these radio frequency signals over the air. The widespread availability of low-cost (less than a few hundred dollars) software-defined radio platforms has put radio transmitters and receivers in the hands of the masses. Although not a necessary condition, in the case of single-tone, the knowledge of the flight’s approach path, the airplane’s manufacturer and model will allow the attacker to significantly optimize their attack signal. We do not restrict the location of the attacker and discuss pros and cons of both an on-board attacker as well as a attacker on the ground.

3.1 Overshadow attack

The overshadow attack is an attack where the attacker transmits specially crafted ILS signals at a power level such that the legitimate signals get overpowered by the attacker’s signal at the receiver. The main reason why such an attack works is that the receivers “lock” and process only the strongest received signal. Figure 3 shows how the attacker’s fake ILS signal completely overshadows the legitimate ILS signal resulting in the deflection of the CDI needle. We note that the attacker signal can be specially crafted to force the CDI needle to indicate a specific offset as demonstrated in Section 4.2.

Attack Signal Generation. Recall that the ILS receiver on-board receives a mix of the transmitted CSB and SBO signals that contain the 90 and 150 Hz tones (Figure 2). The amplitude of received 90 and 150 Hz tones depends on the position of the aircraft relative to the runway and its approach path

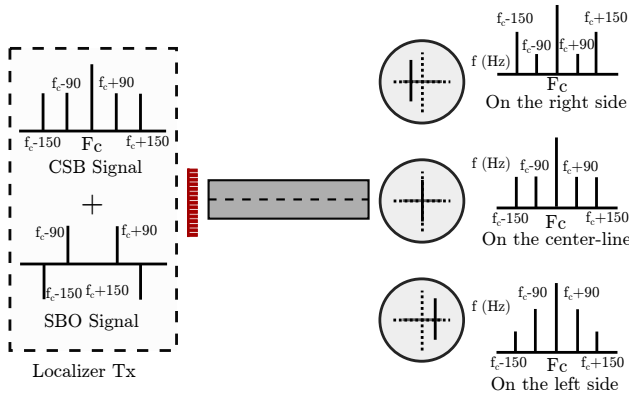


Figure 4: Frequency domain representation of the received signal showing the amplitudes of the sidebands as observed at various lateral offsets

angle. For example, as shown in Figure 4, the 90 Hz tone will dominate if the aircraft is offset to the left of the runway and the 150 Hz dominates to the right. Similarly, for glideslope, the 90 Hz tone dominates glide angles steeper than the recommended angle, and the 150 Hz tone dominates otherwise. Both 90 and 150 Hz will have equal amplitudes for a perfectly aligned approach. Therefore, to execute an overshadow attack, it is sufficient to generate signals similar to the received legitimate ILS signals and transmit at a much higher power as compared to legitimate ILS signals. In other words, the attacker need not generate CSB and SBO signals separately; instead can directly transmit the combined signal with appropriate amplitude differences between the 90 and 150 Hz tones. The amplitude differences are calculated based on the offset the attacker intends to introduce at the aircraft. The attacker's signal (Figure 5) is generated as follows. There are two tone generators for generating the 90 and the 150 Hz signals. It is important to enable configuration of each individual tone's amplitude to construct signals with a preset difference in the depth of modulation corresponding to the required deviation to spoof. The tones are then added and amplitude modulated using the runway's specific localizer or glideslope frequency. Recall that the amplitude differences i.e., difference in depth of modulation (DDM) between the two tones directly corresponds to the required offset to spoof. In the absence of the adversarial signals the estimated $DDM = V_{LOC90} - V_{LOC150}$. In the presence of the attacker's spoofing signals, the estimated $DDM = [V_{LOC90} + V_{AT90}] - [V_{LOC150} + V_{AT150}]$. Since $V_{AT90} \gg V_{LOC90}$ and $V_{AT150} \gg V_{LOC150}$, the resulting $DDM = V_{AT90} - V_{AT150}$. Thus by manipulating the amplitude differences between the transmitted 90 Hz and 150 Hz tones, the attacker can acquire precise control of the aircraft's course deviation indicator and the aircraft's approach path itself.

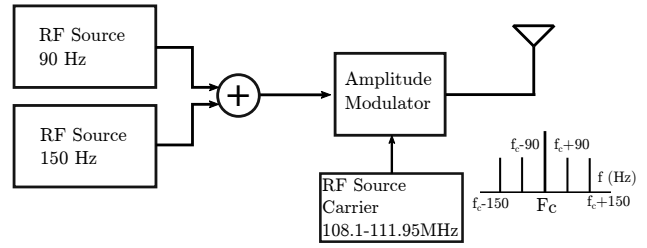


Figure 5: Signal generator used for generating the required attack signal with specific amplitudes of the 90 Hz and 150 Hz components

3.2 Single-tone attack

Single-tone attack is an attack where the attacker transmits only one of the sideband tones (either the 90 Hz or the 150 Hz) to cause deflections in the course deviation indicator needle. In contrast to the overshadow attack, single-tone attack does not require high powered spoofing signals. Recall that the aircraft's horizontal and vertical offset is estimated based on the difference in the depth of the modulation of the 90 Hz and the 150 Hz tones. As indicated in Figure 4, depending on the offset either of the frequency tones dominates. In the case of an overshadow attack, the spoofing signal was constructed with all the necessary frequency components. However, in the single-tone attack, the attacker aims to interfere with only one of the two sideband frequencies directly affecting the estimated offset.

Attack Signal Generation. The working of the single-tone attack is shown in Figure 6. The legitimate localizer signal's spectrum contains the carrier and both the sideband tones of 90 Hz and 150 Hz. As described previously, the amplitudes of the sideband tones depend on the true offset of the aircraft. In a single-tone attack, the attacker generates only one of the two sideband tones i.e., $f_c \pm 90$ or $f_c \pm 150$ with appropriate amplitude levels depending on the spoofing offset (e.g., left or right off the runway) introduced at the aircraft. For example, consider the scenario where the attacker intends to force the aircraft to land on the left of the runway with an offset of 0.5° . The legitimate difference in depth of modulation will be zero as the aircraft is centered over the runway. To cause the aircraft to go left, the attacker must transmit signals that will spoof the current offset to be at the right side of the runway. As shown in Figure 4, the 150 Hz component dominates in the right side of the runway approach and therefore the attacker needs to transmit the $f_c \pm 150$ signal with an appropriate amplitude to force the aircraft to turn left. For the specific example of 0.5° offset, the amplitude of the $f_c \pm 150$ component should be such that the difference in the depth of modulation equals 0.03 [20].

Notice that the single-tone attack signal is similar to a double-sideband suppressed-carrier signal which is well-

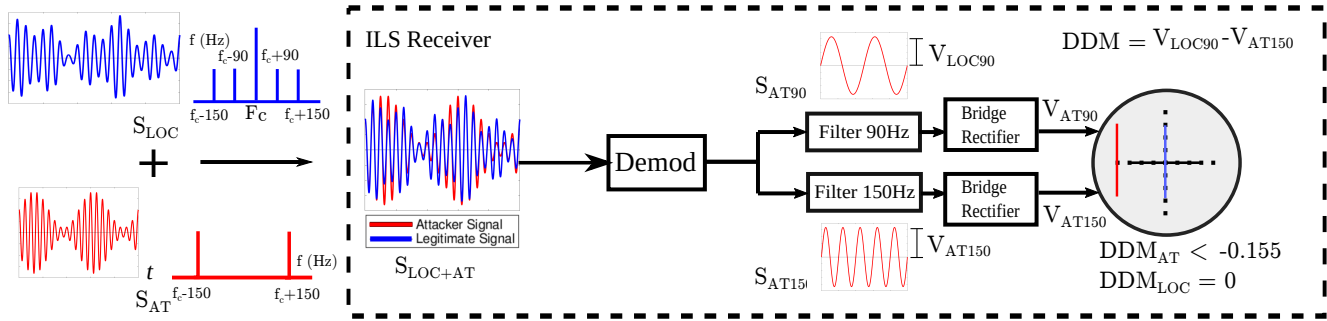


Figure 6: Schematic of the single-tone attack. Attacker constructs a DSB-SC signal without the 90 Hz component and the carrier. The blue line represents the needle position without the attack

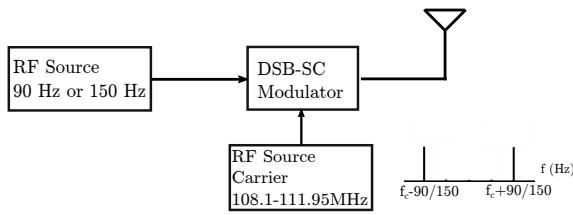


Figure 7: Single-tone attack signal generator with a DSB-SC modulator

known to be spectrally efficient than the normal amplitude modulation signal. Specifically, it is possible for the attacker to reduce the required power to almost 50% of the overshadow attack as there is no need to transmit the carrier signal and one of the sideband signals. One of the important limitations of the single-tone is the effect of the attacker's synchronization with the legitimate signal. To precisely control the spoofing offset, the attacker needs to coarsely control the spoofing signal such that the phase difference between the attacker and the legitimate signals remain constant throughout the attack. We evaluate and show in Section 4.3.1 the effect of phase synchronization on this attack. Additionally, the spectral efficiency of the single-tone attack can be exploited to execute a low-power last-minute denial of service on the ILS system. This is specifically dangerous while an aircraft is executing an auto-pilot assisted approach. The block diagram of the single-tone attack signal generator is shown in Figure 7.

4 Implementation and Evaluation of Attacks

In this section, we demonstrate the feasibility and evaluate the effectiveness of the attack with the help of both simulations and actual experiments conducted using commercial aviation-grade receivers and an advanced flight simulator qualified for FAA certification.

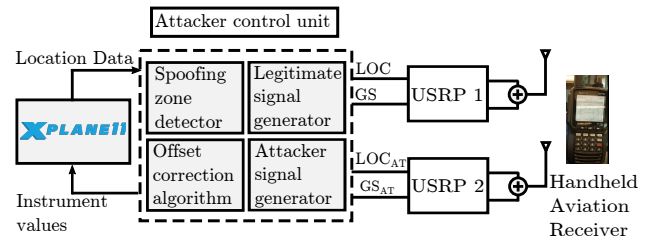


Figure 8: Schematic of the experiment setup used for evaluating the attacks on ILS. The attacker control unit interfaces with the simulator and USRP B210s. A flight yoke and throttle system is connected to the machine running X-Plane flight simulator software. Attacker control unit interfaces with the flight simulator over a UDP/IP network.

4.1 Experimental Setup

Our experimental setup is shown in Figure 8 and Figure 9. The setup consists of four main components: i) X-Plane 11 flight simulator, ii) attacker control unit, iii) software-defined radio hardware platforms (USRP B210s) and iv) commercial aviation grade handheld navigation receiver. We use X-Plane 11 flight simulator to test the effects of spoofing attack on the ILS. X-Plane is a professional flight simulator capable of simulating several commercial, military, and other aircraft. X-Plane can also simulate various visibility conditions and implements advanced aerodynamic models to predict an aircraft's performance in abnormal conditions. It is important to note that X-Plane qualifies for FAA-certified flight training hours when used with computer systems that meet the FAA's minimum frame rate requirements. The certified versions of the software are used in numerous pilot training schools. X-Plane allows interaction with the simulator and instruments through a variety of mobile apps and UDP/IP networks. This feature allowed us to manipulate the instrument readings for evaluating our ILS attacks. Additionally, X-Plane has autopilot

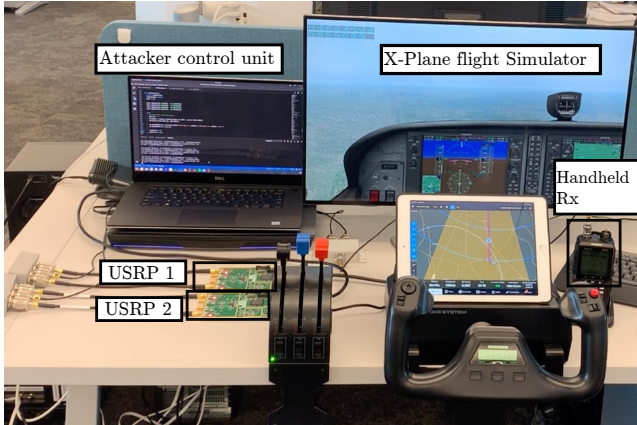


Figure 9: Photo of the experiment setup.

lot and AI-based autoland features which we leverage in our experiments. In other words, X-Plane contains all the features and flexibility to evaluate our proposed attacks in a close to the real-world setting. The second component of our setup is the attacker control unit module which takes the location of the aircraft as input from X-Plane and generates signals for the attack. The module is also responsible for manipulating X-Plane’s instrument panel based on the effect of the spoofing signal on the receiver. The attacker control unit module is a laptop running Ubuntu and contains four submodules: spoofing zone detector, offset correction algorithm, legitimate signal generator, and attacker signal generator. The spoofing zone detector identifies whether an aircraft is entering its first waypoint of the final approach and triggers the start of spoofing. The spoofing zone detector plays an important role in timely starting of the spoofing attack so as to prevent any abrupt changes in the instrument panel and therefore avoid suspicion. The offset correction algorithm uses the current location of the aircraft to continuously correct its spoofing signals taking into consideration aircraft’s corrective actions. Note that the location data received from X-Plane can be analogous to receiving the location data through ADS-B signals [29] in the real world. The output of the offset correction algorithm is used to generate fake ILS signals. We also generate legitimate signals to evaluate the effect of overshadow and single-tone attacks. We use two USRP B210s [2], one each for transmitting legitimate ILS signals and attacker signals. We conducted the experiments in both wired and wireless settings. For the experiments conducted in wireless settings, the receiver was placed at a distance of 2 meters from the transmitter. Northeastern University has access to a Department of Homeland Security laboratory which provides RF shielding thus preventing signal leakage. This is necessary as it is illegal to transmit ILS signals over the air. We use two different ILS receivers, a Yaesu FTA-750L [10] and a Sporty’s SP-400 Handheld NAV/COM Aviation [3] to evaluate the attacks.

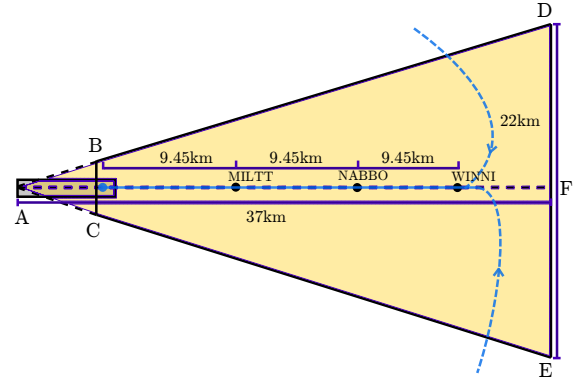


Figure 10: The spoofing zone is defined by points B, C, D, and E. WINNI, NABBO, and MILTT are the waypoints for the final approach as published for a mid-sized airport. The spoofing zone has a wide aperture as the air-traffic controller can vector in the aircraft onto the final approach in multiple ways.

4.1.1 Spoofing Zone Detection

The spoofing zone detection algorithm enables automated and timely triggering of the spoofing signal. One of the key requirements of the zone detector is to trigger the spoofing signals without causing any abrupt changes to the instrument readings; thereby avoiding detection by the pilots. The spoofing region is shaped like a triangle following the coverage of the localizer and glideslope signals. For example, the localizer covers 17.5° on either side of the extended runway centerline and extends for about 35 km beyond the touchdown zone. Figure 10 shows the zone measurements. The attacker signals are triggered when the aircraft approaches the shaded region. The shaded region is decided based on the final approach patterns for a specific runway. We used even-odd algorithm [27] for detecting the presence of the aircraft within this spoofing zone. Absolute locations cannot be used as aircraft enter the final approach path in many different ways based on their arrival direction and air traffic controller instructions. The even-odd algorithm is extensively used in graphics software for region detection and has low computational overhead. The attacker automatically starts transmitting the signals as soon as the aircraft enters the spoofing region from the sides and the needle is yet to be centered. This prevents any sudden noticeable jumps thus allowing a seamless takeover.

4.1.2 Offset correction algorithm

The attacker’s signals are pre-crafted to cause the aircraft to land with a specific offset without being detected. The pilot or the autopilot system will perform course correction maneuvers to align with the runway centerline based on the instrument readings. At this point, the instruments will continuously indicate the spoofed offset irrespective of the aircraft’s location and maneuvers raising suspicion of an instrument failure. To prevent this, we developed a real-time offset correc-

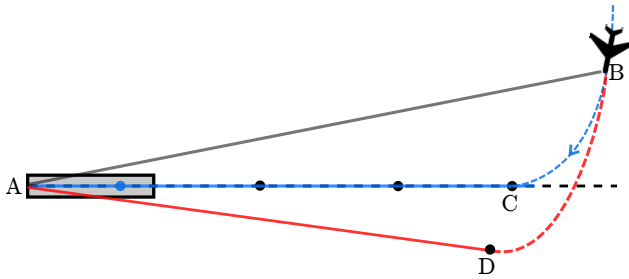


Figure 11: Offset correction algorithm takes into account aircraft’s current position to calculate the difference in the spoofed offset and the current offset.

tion and signal generation algorithm that crafts the spoofing signals based on the aircraft’s current location in real-time. The attacker can use the GPS coordinates if present inside the aircraft or leverage the ADS-B packets containing location information on the ground. We explain the offset correction algorithm using Figure 11. Consider an aircraft at point B, cleared to land and entering the spoofing zone. The air-traffic controller instructs the aircraft to intercept point C on the extended runway centerline. Assuming that the attacker’s spoofing signal contains a pre-crafted offset to the left of the runway forcing the aircraft to follow path DA instead of CA. The offset correction module computes the current offset of the aircraft with respect to the centerline and subtracts the current offset from the spoofed offset to estimate the desired change in the course. Thus, the correction Δ required to be introduced is the difference between required offset angle $\angle DAC$ and the current offset angle $\angle BAC$. Note that offsets to the left of centerline are considered negative offsets and offsets to the right are considered positive offsets. The current offset θ can be estimated using $\theta = \tan^{-1}[(m_{CA} - m_{BA}) / (1 + m_{BA} * m_{CA})]$, where m is the slope. m_{CA} is typically hardcoded and is specific for each runway. m_{BA} can be estimated using the longitude and latitudes of the touchdown point and the current location of the aircraft. Now, the correction Δ is converted to the respective difference in depth of modulation value using the formula $DDM = (DDM_{fullscale} * \Delta) / 2.5$, where 2.5 is the angle that results in full-scale deviation and $DDM_{fullscale}$ is the difference in depth of modulation that causes full-scale deviation. The amplitude of the individual 90 and 150 Hz components is estimated using the formula $0.2 + (DDM / 2)$ and sent to the signal generator module which then transmits the required signal. Note that the value 0.2 comes from the legitimate signal’s depth of modulation. The algorithm was implemented on a laptop running Ubuntu and took less than 5 ms on average to compute the offsets. The complete algorithm is shown in Algorithm 1.

Algorithm 1 Offset correction algorithm.

```

1: procedure GETANGLEDIFFERENCE
2:    $\angle DAC \leftarrow TargetedLocalizerOffset$ 
3:    $\angle BAC \leftarrow GetAngle(location)$ 
4:    $difference \leftarrow \angle DAC - \angle BAC$ 
5:   return  $difference$ 
6: procedure CALCULATEDDM
7:    $difference \leftarrow GetAngleDifference$ 
8:    $ddm \leftarrow (0.155 * difference) / 2.5$ 
9:    $AT90 \leftarrow 0.2 + (ddm) / 2$ 
10:   $AT150 \leftarrow 0.2 - (ddm) / 2$ 
11:   $ChangeAmplitude(AT90, AT150)$ 

```

4.1.3 Setup Validation

We verified the working of our experimental setup as follows. First, we ensure consistency between the CDI needle displayed on the flight simulator and the handheld receiver. To this extent, we disabled the attacker signal and output only the legitimate signal to the handheld receiver based on the aircraft’s location obtained from X-Plane. We manually validated that the alignment shown on the handheld receiver is the same as that of the flight simulator throughout the final approach. The uploaded attack demonstration video ² also contains this validation for reference. We conducted the same experiment over the air in a controlled environment and verified consistency between the handheld receiver and the flight simulator cockpit. Second, we test our offset correction algorithm by maneuvering (swaying) the aircraft during its final approach. During this experiment, the offset correction algorithm should account for the maneuvers and generate corresponding ILS signals to the handheld receiver. We ensure the correctness of the algorithm by validating the consistency between the handheld receiver’s CDI needle and the flight simulator cockpit. Note that we do not update the flight simulator’s instrument readings for this experiment and the readings displayed in the simulator cockpit are only because of the simulator software engine. Finally, we validate the spoofing zone detector algorithm by entering the final approach from various directions and checking the trigger for beginning the spoofing attack. We are now ready to perform our attack evaluations.

4.2 Evaluation of Overshadow Attack

We evaluate the effectiveness of overshadow attack as follows. We leverage the autopilot and autoland feature of X-Plane to analyze the attack’s effects avoiding any inconsistency that might arise due to human error. We configured X-Plane to land on the runway of a midsized airport in the US. This configuration is analogous to the pilot following approach instructions from the air-traffic controller. As soon as the aircraft entered the spoofing zone, the spoofing signals were transmitted along with the legitimate signals. The spoofing

²Video demonstration of the attack <https://youtu.be/Wp4CpyxYJq4>

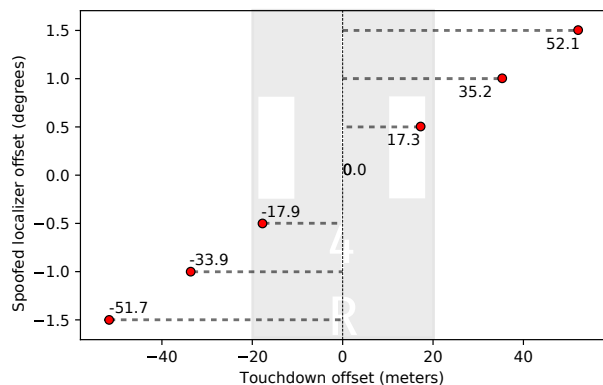


Figure 12: Results of localizer spoofing. 5 automated landings per spoofed localizer offset were executed and the touchdown offset in meters from the runway centerline was recorded.

signals were generated to fake various vertical and horizontal offsets. Note that the spoofing signals were generated in real-time based on the current position of the aircraft. For the localizer (horizontal offset), spoofing signals corresponding to 0.5, 1.0, and 1.5° offset on both sides of the runway were generated. The spoofing glideslope angles were between 2.8° and 3.3°. For each spoofing angle and offset, we performed five automated landings and the results are shown in Figure 12 and Figure 13. Throughout the attack, we continuously monitored the path of the aircraft using Foreflight³, a popular app used both by aviation enthusiasts and commercial pilots as well as X-Plane’s own interfaces. We did not observe any abrupt changes in the readings and observed a smooth takeover. The aircraft landed with an 18 m offset from the runway centerline for a spoofing offset of just 0.5°. Note that this is already close to the edge of the runway and potentially go undetected by both the air-traffic controllers as well as pilots onboard, especially in low visibility conditions. In the case of glideslope, a shift in the glide path angle by 0.1° i.e., 2.9° glide path angle instead of the recommended 3°, caused the aircraft to land almost 800 m beyond the safe touchdown zone of the runway. We have uploaded a video demonstration of the attack for reference (<https://youtu.be/Wp4CpyxYJq4>).

4.3 Evaluation of Single-tone Attack

We evaluate the effectiveness and feasibility of the proposed single-tone attack using the experimental setup described in Section 4.1. Recall that in the single-tone attack, the attacker transmits only one of the sideband tones (either the $f_c \pm 90$ or the $f_c \pm 150$ Hz) to cause deflections in the course deviation indicator needle. We implemented the attack by configuring one of the USRPs (attacker) to transmit the sideband signals and observed its effect on the handheld navigation re-

³Advanced Flight Planner <https://www.foreflight.com>

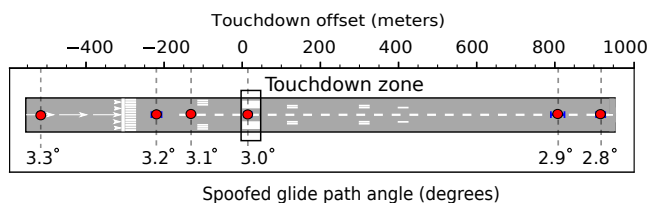


Figure 13: Results of glideslope spoofing. 5 automated landings per spoofed glideslope angle offset were executed and the touchdown offset in meters beyond the touchdown zone was recorded.

ceiver. We observed that the spoofing signal caused the needle to deflect to the configured offset. However, the needle was not as stable as in the overshadow attack and displayed minor oscillations. This is because the specific attack is sensitive to carrier phase oscillations and therefore must be accounted for to avoid detection. A significant advantage of this attack is the power required to cause needle deflections as the attacker only transmits one of the sideband components without the carrier. This gives an almost 50% increase in power efficiency and therefore can act as a low-power last-minute denial of service attack in case the attacker is unable to establish full synchronization with the legitimate signal. In the following sections, we evaluate the effect of phase synchronization on the single-tone attack and develop a real-time amplitude scaling algorithm that can counter the phase oscillations.

4.3.1 Effect of Phase Synchronization

Recall that the single-tone attack signal is similar to a conventional double-sideband suppressed-carrier (DSB-SC) signal. It is well known that one of the drawbacks of a DSB-SC communication system is the complexity of recovering the carrier signal during demodulation. If the carrier signal used at the receiver is not synchronized with the carrier wave used in the generation of the DSB-SC signal, the demodulated signal will be distorted. In the scenario of the single-tone attack, this distortion can potentially result in changes in the difference in the depth of modulation estimates causing the needle to oscillate. We simulated the effect of phase synchronization on the single-tone attack effectiveness and present our results in Figure 14 and Figure 15. We generated the single-tone attack signal to cause full-scale deviation i.e., $\geq 2.5^\circ$ for localizer and $\geq 2.5^\circ$ for the glideslope while perfectly in sync with the legitimate carrier signal. We observe that the phase difference causes the resultant offset to change. We also noted an uncertainty region around the 90° and 270° phase difference region. This is due to the dependency in a DSB-SC system [26] between the carrier phase difference ϕ and the resulting distortion at the output which is directly proportional to the $\cos\phi$. Therefore, at angles around 90° and 270°, there is an uncertainty region for the resulting offset. However, in our experiments on the handheld receiver, we noticed that

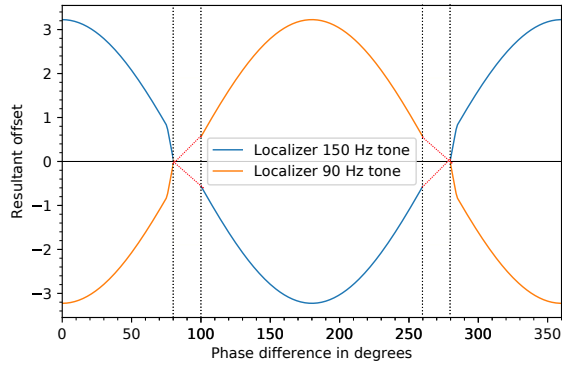


Figure 14: Comparison of calculated offset and the phase difference for localizer

although the needle oscillated, it was not as pronounced as the simulation results indicate. One of the reasons is the rate at which the sensor measurements are being calculated and displayed on the screen. Additionally, the aircraft is in motion, therefore, causing the phase differences to cycle more rapidly than the display’s refresh rate. A knowledgeable attacker can potentially leverage these properties to generate controlled spoofing signals and succeed with an optimized transmission power.

4.3.2 Real-time Amplitude Scaling

In the following, we propose and evaluate a strategy to counter the effect of phase synchronization on the single-tone attack. It is clear that the phase differences cause the output to be distorted. Besides the uncertainty region around the 90° and 270° , it is possible to predict the phase given sufficient knowledge such as aircraft speed, current location, and antenna positions. We assume such a motivated attacker for the single-tone attack evaluation in this section. It is also well known that tightly controlling the phase of a signal is not trivial and therefore our algorithm proposes to manipulate the amplitude of the attacker signal instead of the phase. Changing the amplitude of the attacker signal will compensate for the effect of phase on the signal at the receiver and we call this “real-time amplitude scaling” algorithm. The algorithm itself is inspired from prior works on amplitude scaling for DSB-SC systems [26]. We use the distance between the transmitter and the receiver to estimate the received phase of the signal by measuring complete and incomplete wave-cycles. In the simulation, we then create an ILS signal with the necessary phase shift. We also create the attacker’s signal and add it to the legitimate signal to estimate the DDM. This allows us to assess the impact of phase on the transmitted signal and use this information to calculate the amplitude that will be required to counter the effects of phase. For example, if the predicted phase offset is zero, then to spoof a certain offset, the attacker needs to reduce the amplitude of its signal. We present the results of our amplitude scaling experiment

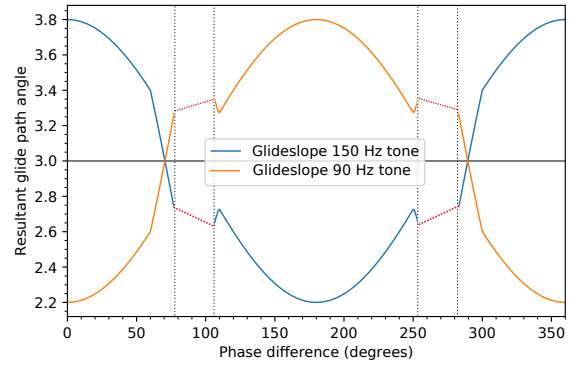


Figure 15: Comparison of calculated offset and the phase difference for glideslope

in Figure 16 and Figure 17.

4.4 Comparison of Power Requirements

One of the major advantages of the single-tone attack is the improvement over the power required to execute the attack, given sufficient knowledge and environmental conditions. In this section, we evaluate and compare the power requirements of the overshadow and the single-tone attacks. We note that the absolute power profiles are specific for the handheld receivers used in the experiments. The goal of the power comparison is to verify whether there is indeed an improvement in terms of attacker’s required transmission power. We present our results in Figure 18 and Figure 19. Our evaluations show the required signal strength to successfully cause 0.5° and 0.1° deviation in localizer and glideslope respectively. The received signal strength profile is shown in blue acts as a reference for the attacker based on which the attacker can compute its required power to transmit the spoofing signals. We performed the experiment by transmitting the signals to the handheld receiver and observing the success of the attack (needle indicating the intended offset). The values are a result of over 400 trials with 95% confidence interval and we find that on an average the difference in power required reaches close to 20.53 dB and 27.47 dB for the localizer and the glideslope respectively. Thus, given sufficient knowledge of the scenario, a motivated attacker can execute the single-tone attack successfully and with less power than the overshadow attack. We acknowledge that the single-tone attack has its drawbacks as described previously, however, we note that given the low power requirements, an attacker can exploit the single-tone attack to cause a low-power denial of service attack. Such an attack, especially in an aircraft’s final moments before landing can be disastrous.

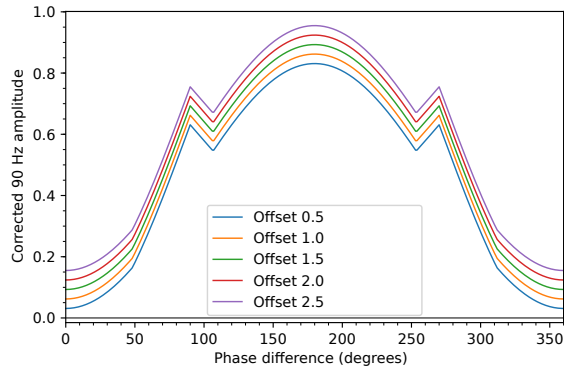


Figure 16: Amplitude scaling algorithm evaluation localizer. Amplitude required to compensate for the effect of phase

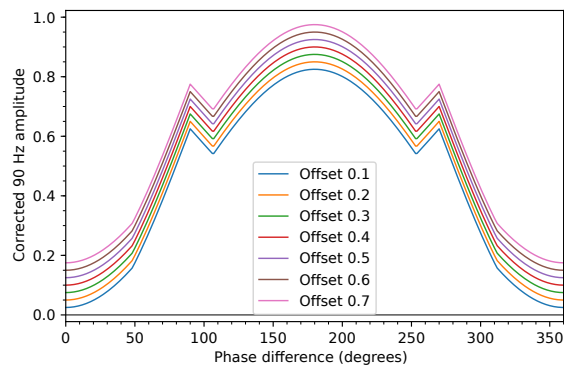


Figure 17: Amplitude scaling algorithm evaluation glideslope. Amplitude required to compensate for the effect of phase

5 Discussion

Receiving antenna characteristics and location of the attacker. The receiver hardware and its characteristics⁴ vary depending on the type of aircraft it is mounted on. For example, Cessna aircraft have their ILS antennas on the tail-fin or the vertical stabilizer. We note that the same antenna is typically used for a number of systems such as VOR, ILS, and DME; each signal arriving from a different direction. For commercial aircraft, the antennas are typically located on the nose of the plane with a forward-looking single broad lobe receiving beam pattern. Certain large aircraft, specifically those capable of landing with high nose attitude, the antennas are located either on the underside or on the landing gear of the aircraft itself⁵. The antenna equipment onboard plays an important role in determining the optimum location of the attacker to execute the attack. The ideal location of an on-ground attacker is at a point along the centerline of the runway

⁴<https://www.easa.europa.eu/certification-specifications/cs-23-normal-utility-aerobatic-and-commuter-aeroplanes>

⁵https://www.casa.gov.au/sites/g/files/net351/f/_assets/main/pilots/download/ils.pdf

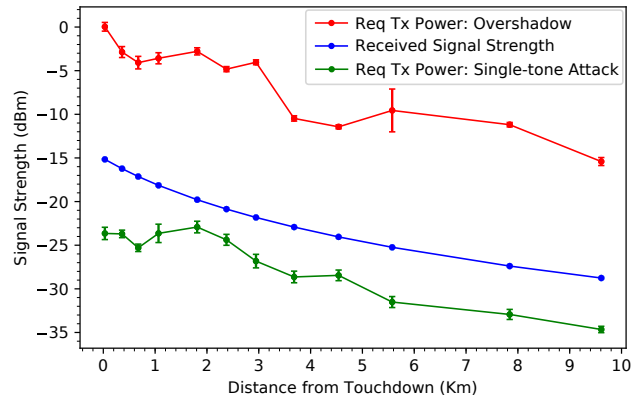


Figure 18: Comparison of required received signal strength for attack methodologies for the localizer

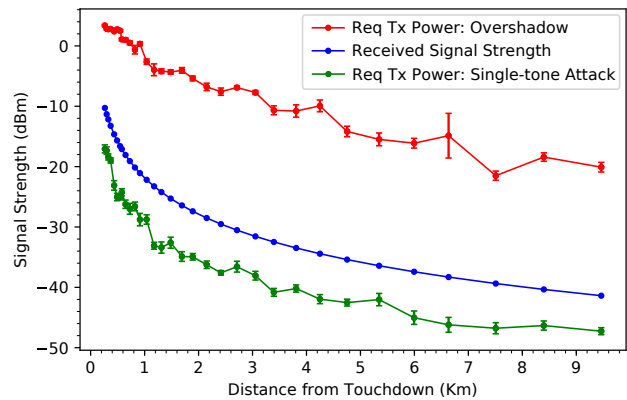


Figure 19: Comparison of required received signal strength for attack methodologies for glideslope

that falls within the receiving lobe of the onboard antennas. Attackers inside the plane will have to deal with signal attenuation caused by the body of the aircraft itself and position the spoofing signal transmitter accordingly. A thorough investigation is required to fully understand the implications and feasibility of an on-board attacker and we intend to pursue the experiments as future work. The location of the attacker plays a more significant role in the scenario of the single-tone attacker since the attacker has to carefully predict the phase and accordingly manipulate the amplitude of the spoofing signal. The problem of identifying optimum locations for the attack is an open problem very similar to the group spoofing problem [56] proposed as a countermeasure for GPS spoofing attacks. In our context, the attacker has to identify locations on the ground such that the phase difference between the legitimate signal and the spoofing signal remains a constant along the line of approach. Recall that in the single-tone attack, the

offset indicated by the cockpit is sensitive to phase changes and therefore locations that allow constant phase differences can result in a fixed spoofing offset and therefore minimal oscillations in the readings.

ILS Categories. The main advantage of ILS is that the pilot need not have visuals of the runway during the final approach as the ILS system is intended to guide the aircraft to a safe landing. The ILS categories are classified based on the maximum decision height at which a missed approach must be initiated if the pilot does not have a visual reference to continue the approach. In CAT I the decision height is at 60 m above the ground i.e., if the pilot does not have a visual reference at this height, a missed approach or go around must be initiated. The decision height for CAT III is as low as 15 m above the ground. The demonstrated attacks can cause severe consequences in CAT III systems due to the low decision height. It might potentially be too late to execute a missed approach in case of an attack. The consequences of the attack on CAT I and CAT II systems are less catastrophic. However, they can still cause major air traffic disruptions. Note that CAT I approach is mostly used by smaller flights. Commercial flights typically fly a CAT II or CAT III approach.

Alternative technologies and potential countermeasures. Many navigation technologies such as HF Omnidirectional Range, Non-directional Beacons, Distance Measurement Equipment and GPS provide guidance to the pilot during the different phases of an aircraft's flight. All the mentioned navigation aids use unauthenticated wireless signals and therefore vulnerable to some form of a spoofing attack. Furthermore, it is worth mentioning that only ILS and GPS are capable of providing precision guidance during the final approach. Also, ILS is the only technology today that provides both lateral and vertical approach guidance and is suitable for CAT III ILS approaches.

Most security issues faced by aviation technologies like ADS-B, ACARS and TCAS can be fixed by implementing cryptographic solutions [50] [52]. However, cryptographic solutions are not sufficient to prevent localization attacks. For example, cryptographically securing GPS signals [24, 33] similar to military navigation can only prevent spoofing attacks to an extent. It would still be possible for an attacker to relay the GPS signals with appropriate timing delays and succeed in a GPS location or time spoofing attack. One can derive inspiration from existing literature on mitigating GPS spoofing attacks [30, 31, 34, 35, 46, 56] and build similar systems that are deployed at the receiver end. An alternative is to implement a wide-area secure localization system based on distance bounding [19] and secure proximity verification techniques [45]. However, this would require bidirectional communication and warrant further investigation with respect to scalability, deployability etc.

Experiment Limitations. Our experimental setup described in Section 4 was carefully constructed in consultation

with aviation experts. Since we use an FAA accredited flight simulator, we sent our configuration files and scripts to a licensed pilot for them to perform final approaches using the instruments and give us feedback. We were mainly concerned whether there was any other indicator on the cockpit that raises suspicion about the attack. We conducted our attack evaluations in both wired and controlled wireless settings. Note that it is illegal to transmit ILS signals over the air in a public space. Effects due to aircraft's motion such as Doppler shift do not affect the attacker signal as these are receiver end problems and the receiver hardware already accounts for such effects for the legitimate signal. Note that the attacker closely imitates the legitimate signals in frequency and amplitude. In short, we made the best effort to replicate a real-world approach. However our setup has its limitations. We did not perform the experiments on a real aircraft which would give us more insights on the effects of aircraft's construction, antenna placements, cockpit display sensitivity, etc. One of the factors that will get affected is the power required by the attacker. Note that commercial ILS transmitters use a 25 watts transmitter for localizer signals and a 5 W power for the glideslope signals. To put things in perspective, a standard 12 V 10 Ah battery can power a 24 Watts amplifier for about 5 hours. Furthermore, we are in touch with a leading aircraft manufacturer for access to such an experiment. We also note that we are in the process of acquiring IRB approval to recruit commercial pilots and studying their response to the attack proposed in this paper.

6 Related Work

Over the years, the aviation industry has largely invested and succeeded in making flying safer. Security was never considered by design as historically the ability to transmit and receive wireless signals required considerable resources and knowledge. However, the widespread availability of powerful and low-cost software-defined radio platforms has altered the threat landscape. In fact, today the majority of wireless systems employed in modern aviation have been shown to be vulnerable to some form of cyber-physical attacks. In this section, we will briefly describe the various attacks demonstrated in prior work. Strohmeier et al. [53] provide a comprehensive analysis of the vulnerabilities and attacks against the various wireless technologies that modern aviation depends on. Voice communication over VHF is primarily used to transfer information between the air traffic controller and the aircraft. There have already been incidents [51] related to spoofed VHF communications and several efforts [23] to design a secure radio communication system. Primary surveillance radars have been shown to be vulnerable to signal jamming attacks [40]. Secondary surveillance radars [6] leverage the ability of the aircraft to respond to ground-based interrogations for aircraft localization. Due to the unauthenticated nature of these messages, it is possible for an attacker to use publicly available implementations for software-defined radio platforms to mod-

ify, inject and jam messages creating a false picture of the airspace. Such attacks were even demonstrated to be low-power, targeted, and stealthy against sophisticated wireless systems such as Wi-Fi [59], and WPA-Enterprise [21]. The ADS-B protocol used by aircraft to transmit key information such as position, velocity and any emergency codes also face the same challenges of active and passive attacks due to the unauthenticated nature of the signals. Several works have repeatedly demonstrated the vulnerabilities of ADS-B signals [7, 18, 22, 38, 47, 48, 52, 54, 60]. ACARS [5], the data link communications system between aircraft and ground stations was found to leak a significant amount of private data [36, 50, 55] e.g., passenger information, medical data and sometimes even credit card details were transferred. Furthermore, an attacker can spoof TCAS messages [42, 48] creating false resolution advisories and forcing the pilot to initiate avoidance maneuvers. For navigation, the aviation industry relies on a number of systems such as ILS, GPS, VOR, and DME. Although the use of VOR and DME are rapidly decreasing, ILS and GPS will be in use for a very long time and are the only technologies available today for enabling autonomous landing. It is also well established that GPS is vulnerable to signal spoofing attacks [11, 13, 32, 39, 41, 56, 61]. Researchers have also demonstrated [43, 44] the feasibility of signal manipulation in the context of data communication systems. However, there has been no prior work on the security guarantees of ILS and this paper is a work in that direction. It is important to note that although many of the security issues in the aviation industry can be fixed by implementing some sort of cryptographic authentication, they are ineffective against the ILS attacks demonstrated in this paper.

7 Conclusion

In this work, we presented a first security evaluation of aircraft instrument landing system against wireless attacks. Through both simulations and experiments using aviation grade commercial ILS receivers and FAA recommended flight simulator, we showed that an attacker can precisely control the approach path of an aircraft without alerting the pilots, especially during low-visibility conditions. We discussed potential countermeasures including failsafe systems such as GPS and showed that these systems do not provide sufficient security guarantees and there are unique challenges to realizing a scalable and secure aircraft landing system.

Acknowledgements

This work was partially supported by NSF grants 1850264, 502481, and 502494. We thank civil air patrol volunteer Vaibhav Sharma for his valuable feedback.

References

- [1] Air Traffic Activity System (ATADS). <https://aspm.faa.gov/opsnet/sys/Airport.asp>.
- [2] Ettus research llc. <http://www.ettus.com/>.

- [3] Sporty's SP-400 Handheld NAV/COM Aviation Radio.
- [4] Aircraft serious incident report occurrences number 00/2518 b767-319er zk-ncj, Civil Aviation Authority of New Zealand, 2002.
- [5] Introduction to ACARS Messaging Services, International Communications Group, April 2006. <https://www.icao.int/safety/acp/inactive%20working%20groups%20library/acp-wg-m-iridium-7/ird-swg07-wp08%20-%20acars%20app%20note.pdf>.
- [6] Aeronautical Telecommunications - Surveillance and Collision Avoidance Systems, International Civil Aviation Organization, 2007. <https://store.icao.int/>.
- [7] Forget any security concern and welcome Air Force One on Flightradar24!, 2011. <https://theaviationist.com/2011/11/24/af1-adsb>.
- [8] Status Report BFU EX010-11, German Federal Bureau of Aircraft Accident Investigation, 2011.
- [9] Acceptable Means of Compliance and Guidance Material to Part-SERA, European Aviation Safety Agency, Sep 2012. <https://www.easa.europa.eu/sites/default/files/dfu/NPA%202012-14.pdf>.
- [10] Yaesu FTA-750L, 2012. <https://www.yaesu.com/airband/indexVS.cfm?cmd=DisplayProducts&DivisionID=2&ProdCatID=204&ProdID=1777>.
- [11] UT Austin Researchers Successfully Spoof an \$80 million Yacht at Sea, 2013. <http://news.utexas.edu/2013/07/29/ut-austin-researchers-successfully-spoof-an-80-million-yacht-at-sea>.
- [12] Stick shaker warning on ILS final, June 2014. <https://www.onderzoeksraad.nl/en/onderzoek/1949/stick-shaker-warning-on-ils-final>.
- [13] Hacking A Phone's GPS May Have Just Got Easier, 2015. <http://www.forbes.com/sites/parmyolson/2015/08/07/gps-spoofing-hackers-defcon/>.
- [14] Air Traffic By The Numbers, Nov 2017. https://www.faa.gov/air_traffic/by_the_numbers.
- [15] Hawker Siddeley HS121 Trident, 2017. <https://www.baesystems.com/en/heritage/hawker-siddeley-hs121-trident>.
- [16] Statistical Summary of Commercial Jet Airplane Accidents Worldwide Operations | 1959 – 2016, Boeing, 2017. www.boeing.com/news/techissues/pdf/statsum.pdf.

- [17] Aeronautical Telecommunications - Radio Navigational Aids, Volume 1, 2018. <https://store.icao.int/>.
- [18] Paul Berthier, José M Fernandez, and Jean-Marc Robert. Sat: Security in the air using tesla. In *Proceedings of the IEEE/AIAA 36th Digital Avionics Systems Conference (DASC)*, 2017.
- [19] Stefan Brands and David Chaum. Distance-bounding protocols. In *Workshop on the theory and application of cryptographic techniques on Advances in cryptology*, 1993.
- [20] Capt. Dennis M. McCollum. Evaluation of Instrument Landing System DDM Calibration Accuracies, 1983. <http://www.dtic.mil/dtic/tr/fulltext/u2/a138301.pdf>.
- [21] Aldo Cassola, William Robertson, Engin Kirda, and Guevara Noubir. A practical, targeted, and stealthy attack against WPA-Enterprise authentication. In *Proceedings of the 20th Annual Network & Distributed System Security Symposium, NDSS'13*, 2013.
- [22] Andrei Costin and Aurélien Francillon. Ghost in the Air (Traffic): On insecurity of ADS-B protocol and practical attacks on ADS-B devices. *BlackHat USA 2012*.
- [23] Romano Fantacci, Simone Menci, Luigia Micciullo, and Laura Pierucci. A secure radio communication system based on an efficient speech watermarking approach. *Proceedings of the Security and Communication Networks*, 2009.
- [24] Ignacio Fernández-Hernández, Vincent Rijmen, Gonzalo Seco-Granados, Javier Simon, Irma Rodríguez, and J David Calle. A Navigation Message Authentication Proposal for the Galileo Open Service. *Navigation*, 2016.
- [25] Booz Allen Hamilton. ASRS - Aviation Safety Reporting System. <https://asrs.arc.nasa.gov>.
- [26] Simon Haykin. *Communication systems*. 2008.
- [27] Kai Hormann and Alexander Agathos. The point in polygon problem for arbitrary polygons. *Computational Geometry*, 2001.
- [28] International Telecommunication Union. *Radio Regulations*. 2012.
- [29] ITU-R - Radiocommunications Sector for ITU. Reception of automatic dependent surveillance broadcast via satellite and compatibility studies with incumbent systems in the frequency band 1 087.7-1 092.3 mhz. 2017.
- [30] Kai Jansen, Matthias Schäfer, Daniel Moser, Vincent Lenders, Christina Pöpper, and Jens Schmitt. Crowd-GPS-sec: Leveraging crowdsourcing to detect and localize GPS spoofing attacks. In *Proceedings of the IEEE Symposium on Security and Privacy (SP)*, 2018.
- [31] Kai Jansen, Nils Ole Tippenhauer, and Christina Pöpper. Multi-receiver GPS spoofing detection: Error models and realization. In *Proceedings of the 32nd Annual Conference on Computer Security Applications*, 2016.
- [32] Roger G. Johnston Jon S. Warner. A Simple Demonstration that the Global Positioning System (GPS) is Vulnerable to Spoofing, 2003. <https://permlink.lanl.gov/object/tr?what=info:lanl-repo/lareport/LA-UR-03-2384>.
- [33] Andrew J Kerns, Kyle D Wesson, and Todd E Humphreys. A blueprint for civil GPS navigation message authentication. In *Proceedings of the IEEE/ION Symposium on Position, Location and Navigation Symposium (PLANS)*, 2014.
- [34] Samer Khanafseh, Naeem Roshan, Steven Langel, Fang-Cheng Chan, Mathieu Joerger, and Boris Pervan. GPS spoofing detection using RAIM with INS coupling. In *Proceedings of the IEEE/ION Symposium on Position, Location and Navigation Symposium (PLANS)*, 2014.
- [35] Brent M Ledvina, William J Bencze, Bryan Galusha, and Issac Miller. An in-line anti-spoofing device for legacy civil GPS receivers. In *Proceedings of the International Technical Meeting of the Institute of Navigation*, 2010.
- [36] Frank Leipold. Session 5: Views of airlines and pilots lufthansa airlines 2014-05-27, May 2014.
- [37] Domenic Magazu III. Exploiting the automatic dependent surveillance-broadcast system via false target injection. Technical report, Air Force Inst of Tech Wright-Patterson AFB OH Dept of Electrical and Computer Engineering, 2012.
- [38] Donald L McCallie. Exploring potential ads-b vulnerabilities in the faa's nextgen air transportation system. Technical report, Air Force Inst of Tech Wright-Patterson AFB OH Dept of Electrical and Computer Engineering, 2011.
- [39] Sashank Narain, Aanjhan Ranganathan, and Guevara Noubir. Security of GPS/INS based on-road location tracking systems. In *Proceedings of the IEEE Symposium on Security and Privacy (SP)*, 2019.
- [40] Naval Air Warfare Center. Electronic warfare and radar systems engineering handbook, 2013. <http://www.navair.navy.mil/nawcaw/ewssa/downloads/nawcaw%20tp%208347.pdf>.

- [41] Tyler Nighswander, Brent M. Ledvina, Jonathan Diamond, Robert Brumley, and David Brumley. GPS software attacks. In *Proceedings of the ACM Conference on Computer and Communications Security*, 2012.
- [42] Pietro Pierpaoli, Magnus Egerstedt, and Amir Rahmani. Altering uav flight path by threatening collision. In *Proceedings of the IEEE/AIAA 34th Digital Avionics Systems Conference (DASC)*, 2015.
- [43] Christina Pöpper, Nils Ole Tippenhauer, Boris Danev, and Srdjan Capkun. Investigation of signal and message manipulations on the wireless channel. In *Proceedings of the European Symposium on Research in Computer Security*, 2011.
- [44] HU Qiao, Yuanzhen Liu, Anjia Yang, and Gerhard Hancke. Preventing overshadowing attacks in self-jamming audio channels. *IEEE Transactions on Dependable and Secure Computing*, 2018.
- [45] Aanjhan Ranganathan and Srdjan Capkun. Are we really close? Verifying proximity in wireless systems. *IEEE Security & Privacy*, 2017.
- [46] Aanjhan Ranganathan, Hildur Ólafsdóttir, and Srdjan Capkun. SPREE: A spoofing resistant GPS receiver. In *Proceedings of the 22nd Annual International Conference on Mobile Computing and Networking*. ACM, 2016.
- [47] Krishna Sampigethaya, Radha Poovendran, and Linda Bushnell. Assessment and mitigation of cyber exploits in future aircraft surveillance. In *Proceedings of the IEEE Aerospace Conference*, 2010.
- [48] Matthias Schäfer, Vincent Lenders, and Ivan Martinovic. Experimental analysis of attacks on next generation air traffic communication. In *Proceedings of the International Conference on Applied Cryptography and Network Security*, 2013.
- [49] Diana Siegel and R John Hansman. Development of an autoland system for general aviation aircraft. Technical report, 2011.
- [50] M. Smith, M. Strohmeier, V. Lenders, and I. Martinovic. On the security and privacy of acars. In *Proceedings of Integrated Communications Navigation and Surveillance (ICNS)*, 2016.
- [51] Tim H Stelkens-Kobsch, Andreas Hasselberg, Thorsten Mühlhausen, Nils Carstengerdes, Michael Finke, and Constantijn Neeteson. Towards a more secure atc voice communications system. In *Proceedings of the IEEE/AIAA 34th Digital Avionics Systems Conference (DASC)*, 2015.
- [52] M. Strohmeier, V. Lenders, and I. Martinovic. On the security of the automatic dependent surveillance-broadcast protocol. *IEEE Communications Surveys Tutorials*, 2015.
- [53] Martin Strohmeier, Matthias Schäfer, Rui Pinheiro, Vincent Lenders, and Ivan Martinovic. On perception and reality in wireless air traffic communication security. *IEEE Transactions on Intelligent Transportation Systems*, 2017.
- [54] Allan Tart and Tõnu Trump. Addressing security issues in ADS-B with robust two dimensional generalized side-lobe canceller. In *Proceedings of 22nd International Conference on Digital Signal Processing (DSP)*, 2017.
- [55] Hugo Teso. Aircraft hacking: Practical aero series. In *Proceedings of HITB Security Conference*, 2013.
- [56] Nils Ole Tippenhauer, Christina Pöpper, Kasper Bonne Rasmussen, and Srdjan Capkun. On the requirements for successful GPS spoofing attacks. In *Proceedings of the 18th ACM Conference on Computer and communications security*, 2011.
- [57] U.S. Department of Transportation. *Nondirectional Beacon (NDB) Installation Standards Handbook*. 1981.
- [58] U.S. Department of Transportation. *Instrument Flying Handbook*. 2012.
- [59] Triet Dang Vo-Huu, Tien Dang Vo-Huu, and Guevara Noubir. Interleaving jamming in Wi-Fi networks. In *Proceedings of the 9th ACM Conference on Security and Privacy in Wireless and Mobile Networks*, 2016.
- [60] Linar Yusupov. ADSB-Out, 2017. <https://github.com/lyusupov/ADSB-Out>.
- [61] Kexiong Curtis Zeng, Shinan Liu, Yuanchao Shu, Dong Wang, Haoyu Li, Yanzhi Dou, Gang Wang, and Yaling Yang. All your GPS are belong to us: Towards stealthy manipulation of road navigation systems. In *Proceedings of the 27th USENIX Security Symposium*, 2018.